Open Access

Journal of Energy and Power Technology

Original Research

Aqueous Lithium--Air Batteries with High Power Density at Room Temperature under Air Atmosphere

Hironari Minami [1], Hiroaki Izumi [1], Takumi Hasegawa [2], Fan Bai [2], Daisuke Mori [2], Sou Taminato [2], Yasuo Takeda [2], Osamu Yamamoto [2,*], Nobuyuki Imanishi [2]

1. Suzuki Motor Corporation, Group 2, Component Engineering Department, Hamamatsu, Shizuoka, 432-8611, Japan; E-Mails: hminami@hhq.suzuki.co.jp; izumih@hhq.suzuki.co.jp
2. Graduate School of Engineering, Mie University, Tsu, Mie, 514-8507, Japan; E-Mails: 421m340@m.mie-u.ac.jp; baifan@mail.sic.ac.cn; daisuke.mori@chem.mie-u.ac.jp; taminato@chem.mie-u.ac.jp; takeda@chem.mie-u.ac.jp; yamamoto@chem.mie-u.ac.jp; imanishi@chem.mie-u.ac.jp

* **Correspondence:** Osamu Yamamoto; E-Mail: yamamoto@chem.mie-u.ac.jp

Academic Editor: Ahamed Irshad

Special Issue: Batteries: Past, Present, and Future

Journal of Energy and Power Technology
2021, volume 3, issue 3
doi:10.21926/jept.2103041

Received: June 30, 2021
Accepted: September 09, 2021
Published: September 23, 2021

Abstract

Rechargeable batteries with higher energy and power density exceeding the performance of the currently available lithium-ion batteries are suitable for application as the power source in electric vehicles (EVs). Aqueous lithium-air batteries are candidates for various EV applications due to their high energy density of 1910 Wh kg^{-1}. The present study reports a rechargeable aqueous lithium-air battery with high power density at room temperature. The battery cell comprised a lithium anode, a non-aqueous anode electrolyte, a water-stable lithium-ion-conducting NASICON type separator, an aqueous catholyte, and an air electrode. The non-aqueous electrolyte served as an interlayer between the lithium anode and the solid electrolyte because the solid electrolyte in contact with lithium was unstable. The mixed separator comprised a Kimwipe paper and a Celgard polypropylene membrane for the interlayer electrolyte, which was used for preventing the formation of lithium dendrites

at a high current density. The proposed aqueous lithium-air battery was successfully cycled at 2 mA cm^{-2} for 6 h at room temperature under an air atmosphere.

Keywords
Aqueous lithium-air battery; high power density; solid electrolyte; lithium dendrite-free; Kimwipe separator

1. Introduction

Electrical vehicles (EVs) release a lower total exhaust carbon dioxide compared to vehicles with internal combustion engines [1]. Therefore, EVs are considered a solution for mitigating the carbon dioxide emissions from conventional vehicles. The main disadvantages of the currently developed EVs are a short driving range and a long charging duration. These problems arise due to the low energy and low power density of conventional lithium-ion batteries, which are used as the power source in EVs currently. However, for the last two decades, various high energy density rechargeable batteries, including non-aqueous lithium-air, aqueous lithium-air, lithium-sulfur, and all-solid-state lithium batteries, are being studied and developed [2-4]. The theoretical energy density values of these battery systems exceed those of the conventional lithium-ion batteries by a significant degree. Nonetheless, these next-generation batteries present serious issues that remain to be resolved, such as the release of water in the air in the case of the non-aqueous lithium-air battery [5], the complexity of the aqueous lithium-air battery system [6], the low cycling performance of the lithium-sulfur battery [7], and the poor contact between the electrolyte and the active electrode in all-solid-state lithium batteries [8].

The theoretical energy density of aqueous lithium-air battery (1910 Wh kg^{-1} and 2004 Wh L^{-1}) is lower than that of the non-aqueous lithium-air system (3458 Wh kg^{-1} and 6170 Wh L^{-1}). However, it is possible to develop an aqueous lithium-air battery with a high specific power density due to the solubility of the cell reaction product (LiOH) in the catholyte [9]. In contrast, the non-aqueous lithium-air battery produces Li_2O_2, which is insoluble in the electrolyte. The deposition of the high-resistance reaction product on the air electrode further blocks the reaction occurring at the electrode. Therefore, in 2004, Visco et al. proposed a rechargeable aqueous lithium-air battery, in which the lithium anode was separated from the aqueous electrolyte using the NASICON-type $Li_{1+x}Al_xTi_{2-x}(PO_4)_3$ to prevent the vigorous reaction between the aqueous solution and the lithium metal [10]. $Li_{1.3}Al_{0.3}Ti_{1.7}(PO_4)_3$ is a lithium-ion-conducting solid electrolyte that remains stable when in contact with water and exhibits a high conductivity of up to 7×10^{-4} S cm^{-1} at 25 °C [11]. Various rechargeable aqueous lithium-air batteries have been reported so far [12-16]. Zhang et al. [15] reported an acid-type aqueous lithium-air battery, with a catholyte comprising acetic acid and lithium acetate, operated at 60 °C. It was expected that this type of battery would have a yield of over 400 Wh kg^{-1}. Sunahiro et al. [16] reported an alkaline-type rechargeable aqueous lithium-air battery with a LiOH-LiCl aqueous solution. The specific energy density calculated using water, lithium, oxygen, and carbon weights in the air electrode was 810 Wh kg^{-1} and the cell performance at room temperature was 0.64 mA cm^{-2}. The aqueous lithium-air battery system has a design of slightly higher complexity compared to the other battery systems with high energy density. This is

because the NASICON-type separator used in the former becomes unstable when it contacts metallic lithium, and an interlayer electrolyte is, therefore, required between the lithium anode and the solid electrolyte separator to prevent direct contact between the solid electrolyte and the lithium metal. This implies that the interlayer electrolyte has to remain stable in contact with both lithium and $Li_{1+x+y}Al_x(Ti, Ge)_{2-x}Si_yP_{3-y}O_{12}$ (LATP). Both Li et al. [17] and Sunahiro et al. [16], in their respective studies, used a conventional non-aqueous electrolyte, such as $LiPF_6$ (or $LiClO_4$) in ethylene carbonate (EC)/diethyl carbonate (DEC). On the other hand, Zhang et al. [15] used a polymer electrolyte based on polyethylene oxide (PEO) in the battery, which then, however, had to be operated at 60 °C as the conductivity of the polymer electrolyte is low at room temperature. In addition to remaining stable when in contact with lithium metal, the interlayer electrolyte also requires preventing the formation of lithium dendrites during the lithium deposition at high current density. Several studies have reported the formation and growth of lithium dendrites when using non-aqueous electrolytes [18-22]. However, Zhang and co-workers reported an electrolyte that did not result in the formation of lithium dendrites even at a high current density; the authors reported that the cell comprised a Li/4 M lithium bis(fluorosulfonyl)imide (LiFSI) in 1,2 dimethyloxyethane (DME)/Li and could be cycled at 10 mA cm^{-2} over a period of 0.1 h for >6,000 cycles [21]. Manthiram and co-workers reported a no-dendrite short circuit for a Li/1.85 M $LiCF_3SO_3$ in DME-1,3 dioxolane (DOL) (1:1 v/v)/Li cell containing a mixed separator composed of Kimwipe paper (KW) and a Celgard porous polypropylene (PP) membrane at 10 mA cm^{-2} for 3 h of 60 cycles [22]. The 4 M LiFSI in DME as a lithium dendrite-free electrolyte and the mixed separator are suitable for application in aqueous lithium-air batteries to be operated under high currents. The present study also reports the performance of an aqueous lithium-air cell with Li/4.5 M LiFSI in DME and a KW and PP/LATP/1.5 M LiOH-10 M LiCl aqueous solution/MnO_2-Ketjenblack (KB), operated at room temperature and a high current density.

2. Experiment

Figure 1 presents a schematic diagram and an image of the aqueous lithium-air test cell. The cell comprised a lithium metal anode, a 4.5 M LFSI in DME serving as an anode side electrolyte, a lithium-ion conducting solid electrolyte, a 1.5 M LiOH-10 M LiCl serving as the cathode side aqueous electrolyte, and an air electrode comprising a mixture of electrolytic MnO_2 and KB. The anode side of the conduction was assembled in an argon-filled glove box and then connected to the cathode side aqueous electrolyte and the air electrode in an air atmosphere. The lithium metal anode (14 × 14 mm; 0.2 mm thick; Honjo Metal, Japan) was packed with a mixed separator composed of KW (50 µm thick; Kimberly-Clark) and PP (25 µm thick; Toray). Both KW and PP were vacuum dried overnight at 60 °C to evaporate water. The NASICON-type solid electrolyte LATP (25 × 25 mm, 0.158 mm thick) was purchased from Ohara Inc., Japan. The room temperature conductivity of LATP was 1.0×10^{-4} S cm^{-1}. A piece of aluminum laminate film (ca. 150 µm thick; Dai Nippon Printing Co. Ltd.) with a square hole (20 × 20 mm) was employed as the sealing film. The cathode side electrolyte was absorbed on an absorbent polymer so that the catholyte would retain water for a longer duration under air. A mixture of electrolytic MnO_2 (300 m^2 g^{-1}; Japan Metal & Chemicals Co. Ltd.), Ketjenblack (KB; Azko Noble), and polytetrafluoroethylene (PTFE; Daikin, Japan) was used as the air electrode to aid conduction. The air electrode mixture comprising 0.853 g MnO_2, 0.24 g PTFE, and 0.107 KB was pressed onto a titanium mesh (25 × 25

mm) by applying a pressure of 20 N. The thickness of the air electrode was approximately 1.0 mm. The full cells were operated at room temperature as well as at 60 °C, under an air atmosphere without airflow.

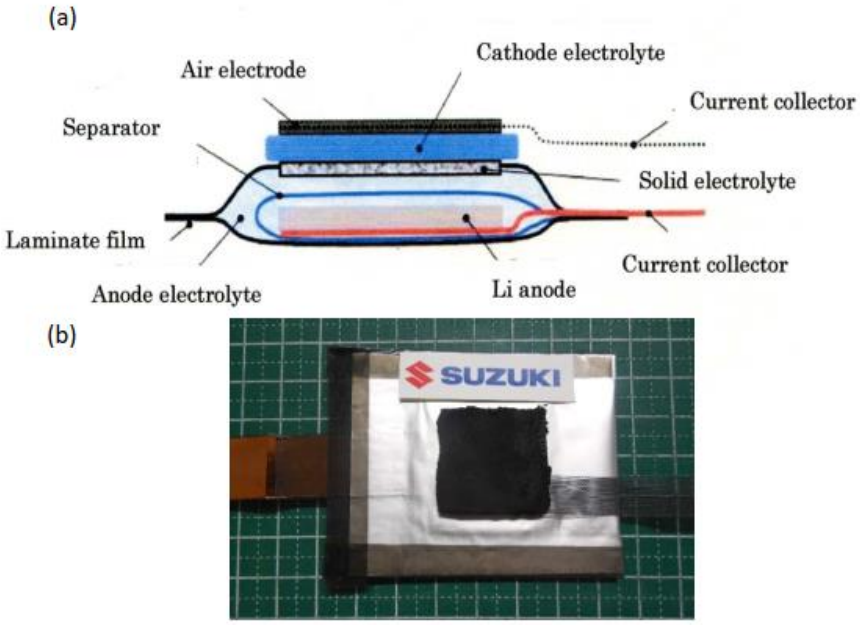

Figure 1 (a) Schematic diagram and (b) image of the lithium-air test cell.

The electrochemical performance of the half-cell was determined under galvanostatic conditions using a battery cycler (BTS 2004H, Nagano). A cell cycling tester (HJ1001 SD8, Hokuto Denko) was employed to measure the charge and discharge performance of the full-cell, and the area of the air electrode was used for calculating the current density of the full cell. Cell impedance was measured using a frequency analyzer (1260, Solartron) in the frequency range of 7 MHz to 0.1 Hz under the applied voltage of 10 mV. Surface morphology was examined using a scanning electron microscope (SEM; S-4000, Hitachi).

3. Results and Discussion

Lithium metal, because of its high specific capacity (3860 mA g^{-1}) and low electrochemical potential (-3.04 V vs. NHE), has been investigated as the anode material for high energy density rechargeable batteries for several years[-]. However, rechargeable batteries with a lithium anode have not been commercialized to date. The reason for this is the formation and growth of lithium dendrite when a rechargeable battery with a lithium anode is operated for longer cycling periods at a high current density [18]. In order to resolve this issue, modified lithium/electrolyte systems that prevent the formation and growth of lithium dendrite [19, 20] have been proposed. In this context, the present study proposes aqueous lithium-air batteries with a 4.5 M LiFSI in DME electrolyte and a mixed separator comprising KW and PP for the anode side electrolyte. Previously, Zhang and co-workers had reported that Li/4 M LiFSI in DME/Li resulted in excellent cycling performance at a high current density [21] along with no lithium dendrite short-circuit at the high current density. In the present study, the 4.5 M LiFSI in DME electrolyte exhibited better cycling

performance in full cells having different contents of LiFSI in DME in the concentration range of 1-5 M of LiFSI. Figure 2 illustrates the galvanostatic cycling performance at 5.0 mA cm^{-2} for 1 h polarization at 25 °C. As depicted in the figure, a steady cycling performance occurs after 10 cycles at 5 mA cm^{-2}. The cell potential was as low as 0.055 V. A low lithium deposition and a low stripping overpotential at a high current density of 5 mA cm^{-2} is preferable for the interlayer electrolyte in the aqueous lithium-air batteries with high power density.

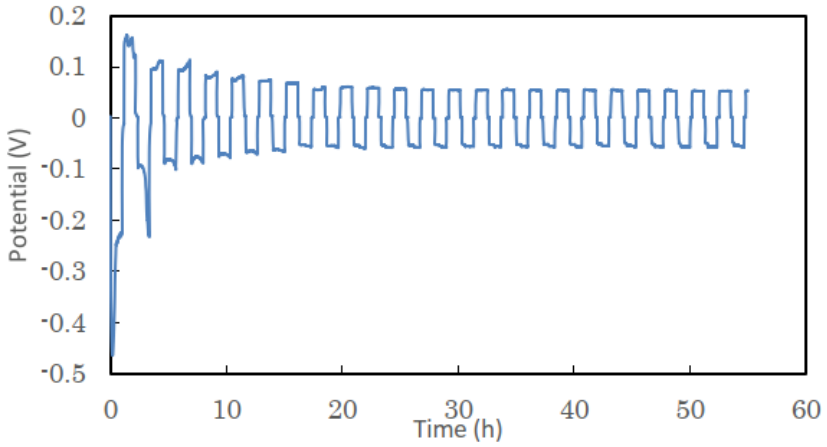

Figure 2 Cycling performance of a cell with Li/4.5 M LiFSI in DME and KW/PP separator/Li at 5.0 mA cm^{-2} and 25 °C.

Another requirement of the lithium electrode is a high coulombic efficiency (CE) for lithium deposition and the stripping reaction. Figure 3 illustrates the dependence of CE on the cycle number of the Li/4.5 M LiFSI in DME/Cu cell with the mixed KW/PP separator, operated at a current density of 1.0 mA cm^{-1} for 1 h polarization and a 1.0 V threshold voltage for stripping [here, CE was simply estimated from the ratio of the plating capacity on the Cu electrode to the stripping capacity from the Cu electrode at a cell voltage of 1.0 V]. The CE gradually increased during the initial several cycles until an average CE of approximately 95% was reached after 20 cycles.

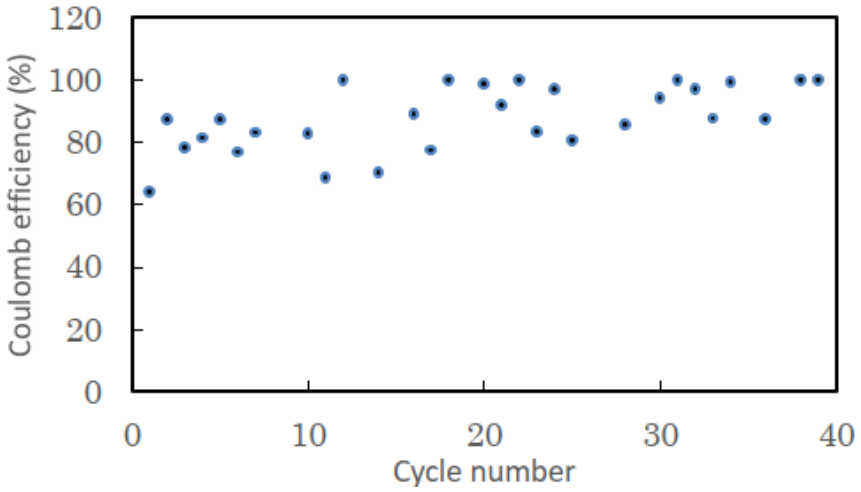

Figure 3 CE for lithium deposition and stripping as a function of cycle number for the Li/4.5 M LiFSI in DME/Cu with the KW/PP separator cell operated at 25 °C and 1.0 mA cm^{-2} for 1 h.

The previously reported non-aqueous lithium-oxygen cells were operated at a low current density of less than 1.0 mA cm^{-2} [23]. Although the aqueous lithium-air cells are expected to operate at a high current density, these cells were also operated at a current density of less than 1.0 mA cm^{-2} in previous studies [23]. For instance, Nemori et al. [24] operated these cells at 0.26 mA cm^{-2}, Sumahiro et al. [16] operated the cells at 0.64 mA cm^{-2}, and Li et al. [25] operated the cells at 0.2 mA cm^{-2}. In the present study, the proposed aqueous lithium-air cells with lithium dendrite-free anodes were operated in air, at room temperature and a high current density of 1.0-2.0 mA cm^{-2} calculated based on the air electrode and that of 2.0-4.0 mA cm^{-2} calculated based on the lithium electrode.

Figure 4 presents the first charge and discharge performance at 1.0 mA cm^{-2} and 25 °C. The current density of 1.0 mA cm^{-2} calculated based on the air electrode area corresponded to the current density of 2.0 mA cm^{-2} calculated based on the lithium electrode area. As depicted in the figure, a steady open-circuit voltage (OCV) of 3.25 V was achieved at 25 °C. The OCV value was similar to the value calculated based on the two-electron reaction $O_2 + H_2O + 2e = HO_2^- + OH^-$ as well as to the values reported previously for the Li/1 M $LiPF_6$ in EC-DEC/Ge doped LATP/saturated LiCl aqueous solution/KB air cell [25] and Li/4 M LiFSI in DME/Nb-doped LATP/10 M LiCl-1.5 M LiOH aqueous solution/MnO_2 air cell [24]. Moreover, the proposed battery demonstrated good charge and discharge performance at 25 °C and 1.0 mA cm^{-2} for 8 h. The round trip overpotential at 1.0 mA cm^{-2} was 0.8 V after 8 h of polarization. The round trip polarization value of this battery at room temperature was considerably lower than the values previously reported for other non-aqueous lithium-air batteries; the values were 1.7 V at 0.64 mA cm^{-2} for the Li/1M $LiClO_4$ in EC/LATP/LiOH-LiCl/RuO_2, air $cell^-$ [16], 1 V at 0.5 mA cm^{-2} for the Li/1M $LiPF_6$ in EC-DEC/LATP/0.1M H_3PO_4-1M LiH_2PO_4/Pt air $cell^-$ [26], and 1.6 V at 0.8 mA cm^{-2} for the Li/[LiFSI-tetraethylene glycol dimethyl ether (G4)]-50 v/v DOL/LAGTP/CH_3COOH/Pt-C air $cell^-$ [27]. The area-specific capacity of 8 mAh cm^{-2}, which corresponds to 41.5 mAh g^{-1} based on the weight of the air electrode determined without the titanium mesh, was higher than the value reported for 1.4 mAh cm^{-2} [26]. The mass capacity of 41.5 mA g^{-1} was considerably lower than that of 210 mAh g^{-1} [26]. The cell impedance decreased with charge and discharge cycling, as depicted in Figure 5. The impedance profiles prior to cycling presented three semicircles: the semicircle in the low-frequency range corresponded to the charge transfer resistances at the lithium and air electrodes, the one in the middle frequency range corresponded to the solid electrolyte interphase (SEI) on the lithium and air electrodes, and the one in the high-frequency range corresponded to the grain boundary resistances of LATP [24, 28, 29]. The equivalent circuit depicted in Figure 5 was used for calculating the total resistance of bulk LATP and liquid electrolyte (R_b), the grain boundary resistance of LAGTP (R_{f1}), the SEI resistance at the anode and the cathode (R_{f2}), and the charge transfer resistance at the anode and the cathode (R_{f3}). The observed R_b of 75 Ω was comparable to that of 60 Ω, as estimated based on the conductivity of LATP and the area of the electrodes. The SEI resistance was considered to be mainly due to the SEI at the lithium electrode as the SEI resistance of 75 Ω (25 Ω cm^2) was comparable to that of 29 Ω cm^2 observed for the Li/4 M LiFSI in DME/Li cell [24]. The charge transfer and SEI resistances were considerably decreased upon charge and discharge cycling, which could be attributed to the 3D lithium electrode formation inside the KW separator, as depicted in Figure 6.

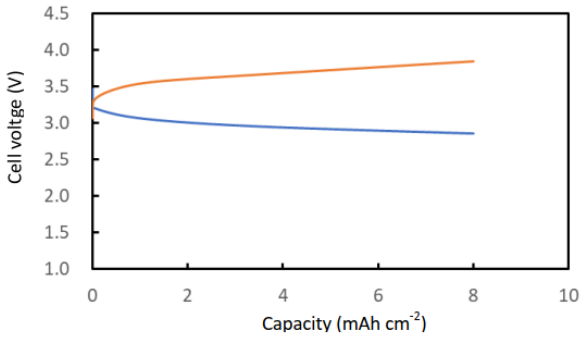

Figure 4 Charge and discharge performance of the Li/4.5 M LiFSI in DME/LATP/1.5 M LiOH-10M LiCl/MnO_2-KB with the KW/PP separator cell at 1.0 cm^{-2} and 25 °C.

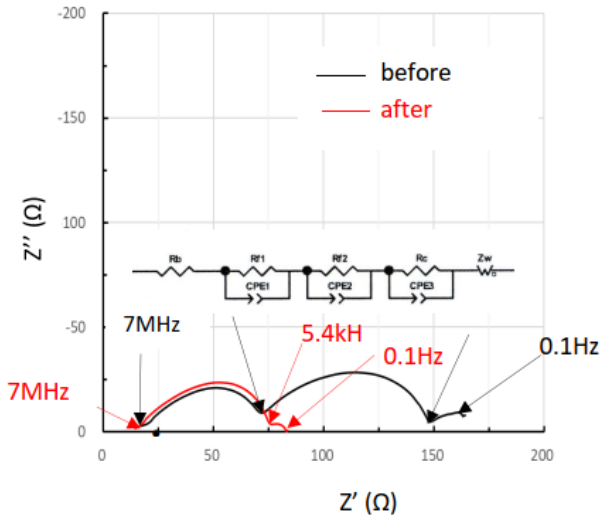

Figure 5 Impedance profiles of the Li/4.5 M LiFSI in DME/LATP/1.5 M LiOH-10 M LiCl/MnO_2-KB air with the KW/PP separator cell prior to and after cycling (4 cycles) at 25 °C and 1.0 cm^{-2} for 8 h.

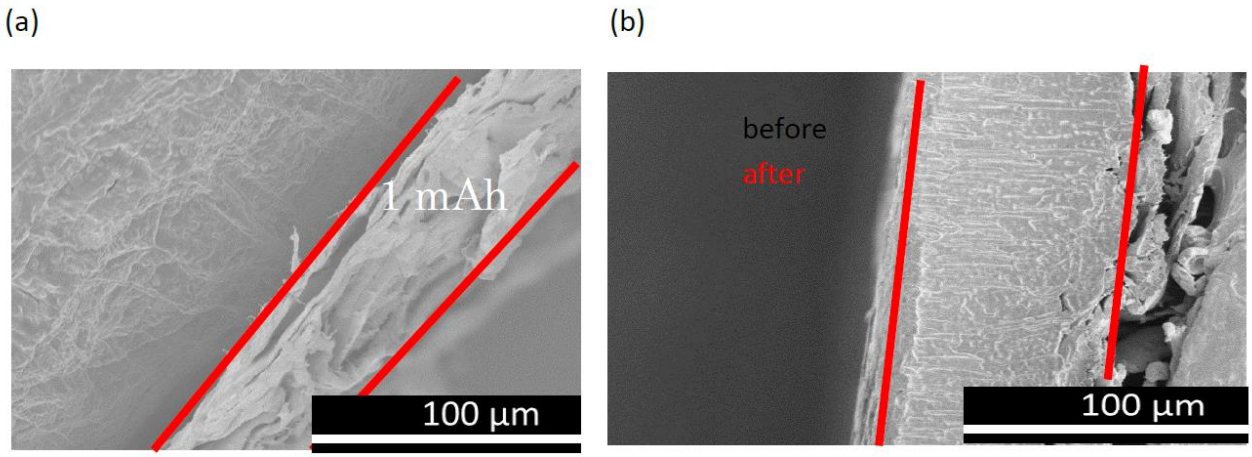

Figure 6 The SEM images of the cross-section of KW after (a) 1 mAh and (b) 47 mAh lithium deposition on a lithium electrode at 1 mA cm^{-2}.

Figure 6 depicts the scanning electron microscopy (SEM) images of the KW cross-section after 1 mAh cm^{-2} and 47 mAh cm^{-2} lithium deposition on the lithium electrode at 1 mA cm^{-2}. The initial 50 µm thickness of KW was expanded to approximately 80 µm after the deposition at 47 mAh cm^{-2}. This increase of approximately 30 µm in thickness was consistent with the thickness of the deposited lithium (22 µm). These results suggested that almost all the lithium was deposited onto the KW separator, i.e., a three-dimensional (3D) lithium electrode had formed in the KW separator. The prevention of dendrite formation at a high current density due to the KW separator could, therefore, be explained by the formation of this 3D lithium electrode inside the KW separator.

Figure 7 presents the cycling performance of the Li/4.5 M LiFSI in DME/LATP/1.5 M LiOH-10 M LiCl/MnO_2-KB air cell for 6 h at 2.0 mA cm^{-2} and 25 °C. In the first 20 cycles, a steady charge and discharge profile was observed, following which the discharge voltage gradually decreased while the charge voltage increased slightly with cycling. The degradation in the cell performance could be attributed to the electrolyte loss at the anode. A total of approximately 2 mL of the anode electrolyte was charged into the test cell. After 20 cycles, this 2 mL of DME was reduced to a volume of 0.35 mL due to reaction with lithium, calculated based on a CE of 95% and the one-electron reaction between lithium and DME. The degradation in the cell performance after cycling could be attributed to the low CE for lithium deposition on and stripping to/from the lithium electrode. Therefore, it is recommended that an electrolyte with a high CE of greater than 99.9% should be developed for lithium deposition and stripping when the cell has to be operated for a longer duration [18]. The current density of the previously reported non-aqueous and aqueous lithium-air batteries was less than 1.0 mA cm^{-2} [23]. Bruce and co-workers [30] reported excellent cycling performance for 2 h at 1.0 mA cm^{-2} using a Li/0.3 M $LiClO_4$ in G4/LATP/0.3 M $LiClO_4$ in DME/carbon nanotube/O_2 cell with double mediators, in which the LATP separator was employed to suppress the reaction of the mediators with the lithium metal anode. The round trip overpotential of this cell was 1.14 V, which was higher than the 0.8 V value obtained for the aqueous lithium-air cell proposed in the present study. The highest current density at 1.0 mA cm^{-2} among all aqueous lithium-air batteries to date has been reported by Bai et al. [31]. The author reported a cell that comprised a lithium anode, a 4.5 M LiFSI in DME interlayer electrolyte at the anode, a $Li_{1.4}Al_{0.4}Ge_{0.2}Ti_{1.4}(PO_4)_3$-10 wt. % TiO_2 separator, a 10 M LiCl-1.5 M LiOH aqueous solution catholyte, and a MnO_2-KB air electrode. The round trip overpotential of this cell at 1.0 mA cm^{-2} was approximately 0.5 V. The cell was successfully cycled for 100 cycles at 1.0 mA cm^{-2} for 1 h polarization. The specific area capacity of the cell was only 1 mAh cm^{-2}, which is less than one-tenth of that obtained for the cell proposed in the present study. Shunahiro et al. also reported the cycling performance of a Li/1M $LiClO_4$ in EC-DEC/LATP/saturated LiOH with 10 M LiCl/KB O_2 cell, which was successfully cycled at 0.64 mA cm^{-2} for approximately 5.8 mAh cm^{-2} for 8 cycles, after, which the discharge potential decreased significantly [16].

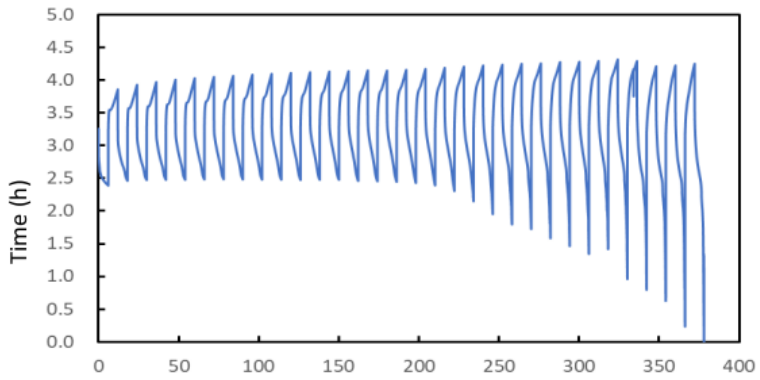

Figure 7 Charge and discharge cycling performance of the Li/4.5 M LiFSI in DME/LATP/1.5 M LiOH-10 M LiCl/MnO_2-KB with the KW/PP separator cell at 2.0 mA cm^{-2} and 25 °C under an air atmosphere.

Furthermore, the cycling performance of the proposed Li/4.5 M LiFSI in DME/LATP/1.5 M LiOH-10 M LiCl/MnO_2-KB with the KW/PP separator cell was evaluated at 60 °C. Figure 8 depicts the cell voltage vs. capacity curves at 2 mA cm^{-2} and 60 °C, for 6 h, as a function of the cycle number. The cell was cycled for 80 cycles. The longer cyclability at 60 °C could be explained by the high CE at a higher temperature. At 60 °C, the estimated CE was approximately 98%, which was higher than the value of approximately 95% obtained at 25 °C.

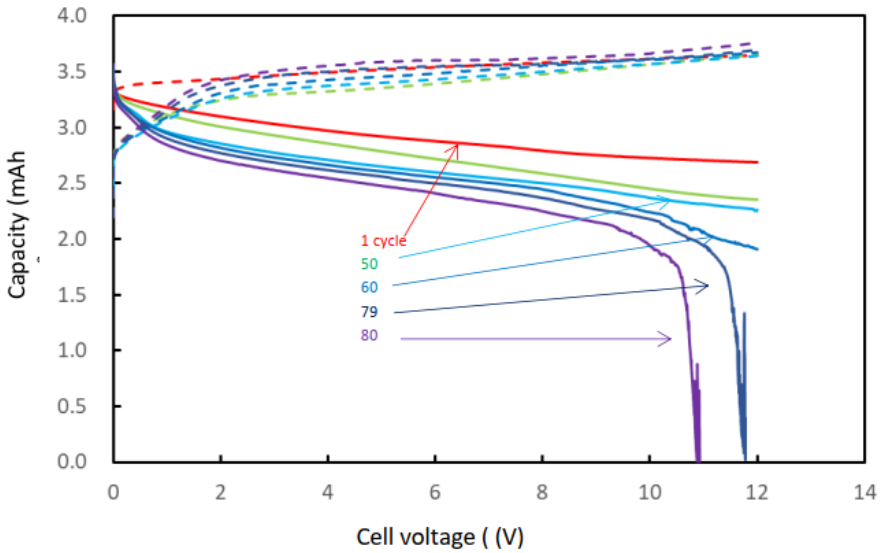

Figure 8 The cell voltage vs. capacity curves for the Li/4.5 M LiFSI in DME/LATP/1.5 M LiOH-10 M LiCl/MnO_2-KB air with the KW/PP separator cell at 2.0 mA cm^{-2} and 60 °C.

Aqueous rechargeable lithium batteries are essentially safe and cost-effective, and are, therefore, considered attractive candidates for application in large-scale energy storage systems. Lead-acid batteries have been used for these applications for over 100 years. However, a major disadvantage of lead-acid batteries is their low energy density. In addition to aqueous lithium-air batteries, several other advanced aqueous rechargeable batteries have been proposed in the last few decades, including the aqueous lithium-metal chloride [32], aqueous lithium-$Fe(CN)_6^{3-}$

/$Fe(CN)_6^{-4-}$ [33], and aqueous Sn/$LiCoPO_4$ [34] batteries [10]. Among these, aqueous lithium-air battery, the one used in the present study as well, is reported with a high energy density of over 500 Wh kg^{-1} [27] and a low round-trip overpotential at a high current density of 2.0 mA cm^{-2}, in air and at room temperature. Nonetheless, a critical change is required in the aqueous lithium-air batteries, i.e., improvement in their coulombic efficiency for lithium deposition and stripping.

4. Conclusion

An aqueous lithium-air rechargeable battery comprising a lithium anode, a 4.5 M LiFSI in DME anolyte with a double separator composed of KW and PP, a LATP solid electrolyte separator, a 1.5 M LiOH-10 M LiCl aqueous solution catholyte, and a MnO_2/KB air electrode was operated at room temperature under an air atmosphere. The battery demonstrated a steady charge and discharge cycle performance for the first 20 cycles at 2 mA cm^{-2} and 12 mAh cm^{-2}. The power density of the proposed battery was the highest among all the lithium-air cells reported to date. The degradation of the cell performance upon long-term cycling could be attributed to the low CE for lithium deposition and stripping in the anolyte. At 60 °C, the cell could be successfully cycled for 70 cycles at 2 mA cm^{-2} and 12 mAh cm^{-2}, with a CE higher than that at 25 °C. Nonetheless, developing a lithium electrode with a higher CE is warranted to ensure the long-term operation of aqueous lithium-air batteries.

Author Contributions

H.M. and H. I. set up the full cells, and performed electrical measurements. T. H. conducted CE measurements. F. B conducted SEM measurements. D. M., S. T., and Y. T. gave advice on each experimental work. H. M., H. I., and O. Y. prepared the manuscript. N. I. managed the research direction.

Competing Interests

The authors have declared that no competing interests exist.

References

1. Girishkumar G, McCloskey B, Luntz AC, Swanson S, Wilcke W. Lithium-air battery: Promise and challenges. J Phys Chem Lett. 2010; 1: 2193-2203.
2. Bruce PG, Freunberger SA, Hardwick LJ, Tarascon JM. Li-O_2 and Li-S batteries with high energy storage. Nat Mater. 2012; 11: 19-29.
3. Armand M, Tarascon JM. Building better batteries. Nature. 2008; 451: 652-657.
4. Kamaya N, Homma K, Yamakawa Y, Hirayama M, Kanno R, Yonemura M, et al. A lithium superionic conductor. Nat Mater. 2011; 10: 682-686.
5. Gallagher KG, Goebel S, Greszler T, Mathias M, Oelerich W, Eroglu D, et al. Quantifying the promise of lithium-air batteries for electric vehicles. Energy Environ Sci. 2014; 7: 1555-1563.
6. Zhang T, Imanishi N, Shimonishi Y, Hirano A, Takeda Y, Yamamoto O, et al. A novel high energy density rechargeable lithium/air battery. ChemComm. 2010; 46: 1661-1663.
7. Varzi A, Thanner K, Scipioni R, Di Lecce D, Hassoun J, Dörfler S, et al. Current status and future perspectives of lithium metal batteries. J Power Sources. 2020; 480: 228803.

8. Ye L, Li X. A dynamic stability design strategy for lithium metal solid state batteries. Nature. 2021; 593: 218-222.
9. Yamamoto O. Introduction. In: The lithium air battery: Fundamentals. New York: Springer; 2013. pp.1-21.
10. Visco SJ, Nimon E, Katz B, De Jonghe LC, Chu MY. Abstract #53. Proceedings of the 12th International Meeting on Lithium Batteries; 2004 June 27th-July 2nd; Nara, Japan. Lausanne: Elsevier.
11. Aono H, Sugimoto E, Sadaaka Y, Imanaka N, Adachi GY. Ionic conductivity of the lithium titanium phosphate ($Li_{1+x}M_xTi_{2-x}(PO_4)_3$, M = Al, Sc, Y, and La) systems. J Electrochem Soc. 1989; 136: 590-591.
12. Imanishi N, Takeda Y, Yamamoto O. Aqueous lithium-air rechargeable batteries. Electrochemistry. 2012; 80: 706-715.
13. Manthiram A, Li L. Hybrid and aqueous lithium-air batteries. Adv Energy Mater. 2015; 5: 1401302.
14. He P, Zhang T, Jiang J, Zhou H. Lithium-air batteries with hybrid electrolytes. J Phys Chem Lett. 2016; 7: 1267-1280.
15. Wang Y, Zhou H. A lithium-air fuel cell using copper to catalyze oxygen-reduction based on copper-corrosion mechanism. Chem Commun. 2010; 46: 6305-6307.
16. Sunahiro S, Matsui M, Takeda Y, Yamamoto O, Imanishi N. Rechargeable aqueous lithium-air batteries with an auxiliary electrode for the oxygen evolution. J Power Sources. 2014; 262: 338-343.
17. Li L, Chai SH, Dai S, Manthiram A. Advanced hybrid Li-air batteries with high-performance mesoporous nanocatalysts. Energy Environ Sci. 2014; 7: 2630-2636.
18. Cheng XB, Zhang R, Zhao CZ, Zhang Q. Toward safe lithium metal anode in rechargeable batteries: A review. Chem Rev. 2017; 117: 10403-10473.
19. Imanishi N, Zhang T, Mori D, Taminato S, Takeda Y. Lithium metal anode for high-power and high-capacity rechargeable batteries. J Energy Power Technol. 2021; 3. Doi: 10.21926/jept.2102019.
20. Wang H, Liu Y, Li Y, Cui Y. Lithium metal anode materials design: Interphase and host. Electrochem Energy Rev. 2019; 2: 509-517.
21. Qian J, Henderson WA, Xu W, Bhattacharya P, Engelhard M, Borodin O, et al. High rate and stable cycling of lithium metal anode. Nat Commun. 2015; 6: 6362.
22. Chang CH, Chung SH, Manthiram A. Dendrite-free lithium anode via a homogenous Li-ion distribution enabled by a Kimwipe paper. Adv Sustain Syst. 2017; 1: 1600034.
23. Imanishi N, Yamamoto O. Perspectives and challenges of rechargeable lithium-air batteries. Mater Today Adv. 2019; 4: 100031.
24. Nemori H, Shang X, Minami H, Mitsuoka S, Nomura M, Sonoki H, et al. Aqueous lithium-air batteries with a lithium-ion conducting solid electrolyte $Li_{1.3}Al_{0.5}Nb_{0.2}Ti_{1.3}(PO_4)_3$. Solid State Ion. 2018; 317: 136-141.
25. Li Y, Huang K, Xing Y. A hybrid Li-air battery with buckypaper air cathode and sulfuric acid electrolyte. Electrochim Acta. 2012; 81: 20-24.
26. Li L, Zhao X, Manthiram A. A dual-electrolyte rechargeable Li-air battery with phosphate buffer catholyte. Electrochem Commun. 2012; 14: 78-81.
27. Soga S, Bai F, Zhang T, Kakimoto K, Mori D, Taminato S, et al. Ambient air operation

rechargeable lithium-air battery with acetic acid catholyte. J Electrochem Soc. 2020; 167: 090522.
28. Zhang P, Wang H, Lee YG, Matsui M, Takeda Y, Yamamoto O, et al. Tape-cast water-stable NASICON-type high lithium ion conducting solid electrolyte films for aqueous lithium-air batteries. J Electrochem Soc. 2015; 162: A1265.
29. Bruce PG, West AR. Ionic conductivity of LISICON solid solutions, $Li_{2+2x}Zn_{1-x}GeO_4$. J Solid State Chem. 1982; 44: 354-365.
30. Gao X, Chen Y, Johnson LR, Jovanov ZP, Bruce PG. A rechargeable lithium-oxygen battery with dual mediators stabilizing the carbon cathode. Nat Energy. 2017; 2: 17118.
31. Bai F, Shang X, Mori D, Taminato S, Matsumoto M, Watanabe S, et al. High lithium-ion conducting solid electrolyte thin film of $Li_{1.4}Al_{0.4}Ge_{0.2}Ti_{1.4}(PO_4)_3$-$TiO_2$ for aqueous lithium secondary batteries. Solid State Ion. 2019; 338: 127-133.
32. Morita Y, Watanabe S, Zhang P, Wang H, Mori D, Matsuda Y, et al. High specific energy density aqueous lithium-metal chloride rechargeable batteries. J Electrochem Soc. 2017; 164: A1958.
33. Lu Y, Goodenough JB, Kim Y. Aqueous cathode for next-generation alkali-ion batteries. J Am Chem Soc. 2011; 133: 5756-5759.
34. Minakshi M, Singh P, Sharma N, Blackford M, Ionescu M. Lithium extraction-insertion from/into $LiCoPO_4$ in aqueous batteries. Ind Eng Chem Res. 2011; 50: 1899-1905.